

Heavy-Tailed Pitman–Yor Mixture Models

Vianey Palacios Ramírez, Miguel de Carvalho, Luis Gutiérrez Inostroza*

November 3, 2022

Abstract

Heavy tails are often found in practice, and yet they are an Achilles heel of a variety of mainstream random probability measures such as the Dirichlet process. The first contribution of this paper focuses on the characterization of the tails of the so-called Pitman–Yor process, which includes the Dirichlet process as a particular case. We show that the right tail of a Pitman–Yor process, known as the stable law process, is heavy-tailed, provided that the centering distribution is itself heavy-tailed. A second contribution of the paper rests on the development of two classes of heavy-tailed mixture models and the assessment of their relative merits. Multivariate extensions of the proposed heavy-tailed mixtures are here devised along with a predictor-dependent version so to learn about the effect of covariates on a multivariate heavy-tailed response. The simulation study suggests that the proposed method performs well in a variety of scenarios, and we showcase the application of the proposed methods in a neuroscience dataset.

Keywords: Bayesian nonparametrics, Bulk, Random probability measure, Stick-breaking prior, Tail index.

1 INTRODUCTION

Thousands of heavy-tailed signals are produced on a day-to-day basis across the globe in fields as diverse as engineering, finance, and medicine. And yet, despite the widespread need for modeling these, heavy tails remain a weak spot of several established random probability measures such as the Dirichlet process (e.g. Ghosal and Van der Vaart, 2015, Section 4.3).

Prior to introducing the main problems to be addressed, and the main contributions of this paper, we first lay the groundwork. The Pitman–Yor process is a random probability measure that has received considerable attention in recent years (e.g. Pitman and Yor, 1997; Ishwaran and James, 2001; Teh, 2006; Bassetti et al., 2014; Miller and Harrison, 2014; Canale et al., 2017; Arbel et al., 2019; Lijoi et al., 2020; Corradin et al., 2021) and that includes the Dirichlet process as a particular case. Some Bayesian nonparametric approaches, such as the Pitman–Yor process, can be understood as an extension of standard parametric methods in the sense that they are centered a priori around a parametric model, $\{G_{0,\theta} : \theta \in \Theta \subseteq \mathbb{R}^q\}$, but assign positive mass to a variety of alternatives.

*V. Palacios Ramírez is a University teacher in Statistics, School of Mathematics, University of Edinburgh (kramirez@ed.ac.uk). M. de Carvalho is Reader in Statistics, School of Mathematics, University of Edinburgh (Miguel.deCarvalho@ed.ac.uk). L. Gutiérrez Inostroza is Assistant Professor in Statistics, Pontificia Universidad Católica de Chile. ANID–Millennium Science Initiative Program–Millennium Nucleus Center for the Discovery of Structures in Complex Data. (llgutier@mat.uc.cl).

Thus, a recurring theme in much of the Bayesian nonparametric literature is to regard a parametric approach—known as the baseline or centering distribution—as a reference, while allowing for other alternative models to take over when data suggests that the parametric model is inappropriate. See the monographs of Müller et al. (2015) and Ghosal and Van der Vaart (2015) or the review paper of Müller and Mitra (2013) for an introduction to Bayesian nonparametric inference.

It is well-known that the tails of the Dirichlet process are exponentially much thinner than those of the baseline (Ghosal and Van der Vaart, 2015, Section 4.2.3). Motivated by this, this paper opens with the question on whether this is simply a property of the Dirichlet process or whether it is more generally an attribute of the Pitman–Yor process. Hence, the first contribution of this paper will focus on the characterization of the tails of the Pitman–Yor process. In particular, we will derive envelopes for the trajectories of the tail of a particular instance of the Pitman–Yor process, known as the stable law process. As will be discussed below (Section 2.1), the latter envelopes combined with those of Doss and Sellke (1982) offer an almost complete portrait of the tails of the Pitman–Yor process. In addition, we then show that the tail of the stable law process is only moderately thinner than that of the baseline; in particular, our results imply that the tail of the stable law process is heavy-tailed, provided that the baseline is itself heavy-tailed. This result is in sharp contrast with the Dirichlet process, given that, as mentioned earlier, its tail is exponentially much lighter than that of the centering.

A second contribution of the paper rests on the development of two classes of heavy-tailed mixture models and the assessment of their relative merits. The heavy-tailed mixture models devised here have links with the phase-type scale mixtures of Bladt and Rojas-Nandayapa (2018) and the infinite mixtures of Pareto distributions of Tressou (2008). Our focus differs however from these papers in several important ways. Some key differences are that we take a general view of heavy-tailed Pitman–Yor mixtures and take advantage of our novel characterization of its tail. In addition, by keeping a general focus in mind, our theoretical and numerical analyses will reveal that there are some good reasons for preferring stable process scale mixtures over Pitman–Yor mixtures build from heavy-tailed kernels. Finally, motivated by the fact that heavy-tailed data are frequently multivariate—and since covariates are often available—we further extend the proposed heavy-tailed scale mixture models to model these as well. In other words, multivariate extensions of the proposed heavy-tailed mixtures are also devised below along with a predictor-dependent version to learn about the effect of covariates on a multivariate heavy-tailed response. A final comment on the jargon of heavy tails is in order. Following the standard convention in the literature on heavy tails (e.g. Resnick, 2007), here we will characterize these via regular variation (Bingham et al., 1989). A distribution function $F(y) = P(Y \leq y)$, or its density $f = dF/dy$ in case it exists, is said to have a regularly varying tail, with tail index $\alpha \equiv \alpha(F) > 0$, if

$$\lim_{y \rightarrow \infty} \frac{P(Y > yt)}{P(Y > y)} = t^{-\alpha}. \quad (1)$$

The smaller the tail index, the slower the decay of the tail, $1 - F(y)$, to 0 as $y \rightarrow \infty$, and thus the more heavy-tailed is the distribution. Throughout, the notation $1 - F \in \text{RV}_{-\alpha}$ is used to denote that F verifies (1).

The remainder of this paper unfolds as follows. In Section 2, we study the tails of the Pitman–Yor process and construct two classes of heavy-tailed Pitman–Yor mixture models. In Section 3 we expand the proposed toolbox to the multivariate setting as well as to a conditional framework. Section 4 illustrates the performance of the proposed methods and reports the main findings of our numerical studies. An application of the proposed methods to a neuroscience case study is given in Section 5. Finally, in Section 6 we present closing remarks. Proofs are available in the Appendix, and further technical details and supporting numerical evidence can be found in the online supporting informa-

tion; the R package `pit Yor`, available from the supporting information, implements instances of the methods proposed herein.

2 HEAVY-TAILED PITMAN–YOR MIXTURE MODELS

2.1 On the tails of the Pitman–Yor process

Subordinator-type representations: We start by studying the tails of the Pitman–Yor process since its properties will be vital for constructing our class of mixture models. The main result of this section is Theorem 2, but before we can discuss its implications, we first lay the groundwork. Recall that a random probability measure G follows a Pitman–Yor process, here denoted as $G \sim \text{PYP}(D, M, G_0)$, if it admits a stick-breaking representation of the type,

$$G = \sum_{h=1}^{\infty} \pi_h \delta_{Y_h}, \quad Y_h \stackrel{\text{iid}}{\sim} G_0. \quad (2)$$

Here, δ_Y denotes a point mass at Y , and the weights are generated by a stick-breaking scheme, that is, $\pi_h = V_h \prod_{k < h} (1 - V_k)$ with $V_h \stackrel{\text{iid}}{\sim} \text{Beta}(1 - D, M + hD)$, for $h \in \mathbb{N} = \{1, 2, \dots\}$. The parameters of the Pitman–Yor process are known as discount (D), precision (M), and centering distribution function (G_0) and are subject to the constraints $0 \leq D < 1$ and $M > -D$. The Dirichlet process, $\text{DP}(M, G_0)$, is a particular case with $D = 0$, and the case $M = 0$ is known as the class of stable law processes, $\text{SP}(D, G_0)$.

In this subsection we will examine the behavior of $1 - G(y)$, as y approaches the right endpoint, $y_+ = \sup\{y : G(y) < 1\}$, where $G(y)$ is the the random distribution function of a $\text{PYP}(D, M, G_0)$. Recall that both $G \sim \text{PYP}(D, M, G_0)$ and G_0 are supported over the same set, and thus the right endpoints of G and G_0 coincide. Following the standard convention in extreme value analysis, we focus on the right tail, but all claims below apply to the left tail with minor adjustments.

While the stick-breaking representation of the Pitman–Yor process in (2) is handy for a variety of contexts, the process also admits subordinator-type representations, which turn out to be more suitable for studying its tails. A subordinator, $\{S(t) : t \geq 0\}$, is an increasing stochastic process over the positive real line that has independent and homogeneous increments (e.g. Applebaum, 2009, Ch. 1). By the so-called Lévy–Khintchine representation (e.g. Bertoin, 1999, Section 1.2), a subordinator is fully characterized by its Laplace exponent,

$$\Phi(\lambda) = k + d\lambda + \int_0^{\infty} (1 - e^{-\lambda u}) \nu(du), \quad \lambda \geq 0,$$

that obeys $E[\exp\{-\lambda S(t)\}] = \exp\{-t\Phi(\lambda)\}$, for $t \geq 0$; here, $k > 0$ is the killing rate, $d > 0$ is the drift coefficient, and ν is a measure on $(0, \infty)$ —known as Lévy measure—that governs the law of the increments and which obeys the constraint $\int_0^{\infty} \min(1, u) \nu(du) < \infty$. It is well-known that both the Dirichlet process and stable law processes admit subordinator representations (e.g. Pitman and Yor, 1997, Propositions 5–6), a fact that we briefly review in the following examples.

Example 1 (Subordinator representation of $\text{PYP}(0, M, G_0)$). If $G \sim \text{DP}(M, G_0)$, then

$$G(y) = \frac{\gamma\{MG_0(y)\}}{\gamma(M)}, \quad y \in \mathbb{R}. \quad (3)$$

See, for instance, Ferguson (1973, 1974) and Ghosal and Van der Vaart (2015, Section 4.2.3). Here, γ is a Gamma process, that is, $k = d = 0$ and $\nu(du) = u \exp(-u) du$, for $u > 0$.

Example 2 (Subordinator representation of $\text{PYP}(D, 0, G_0)$). If $G \sim \text{SP}(D, G_0)$, then

$$G(y) = \frac{S\{G_0(y)\}}{S(1)}, \quad y \in \mathbb{R}. \quad (4)$$

Here, S is a D -stable subordinator, that is, $k = d = 0$ and $\nu(du) = D/\Gamma(1-D)u^{-1-D}$, for $u > 0$, where $\Gamma(z) = \int_0^\infty u^{z-1} \exp(-u) du$ is the gamma function. The stable process representation in (4) is an immediate consequence of Pitman and Yor (1997, Proposition 6).

On the tails of the Pitman–Yor process: The tails of the Dirichlet process are much lighter than those of the centering distribution, with probability one, a fact that can be shown using the representation from Example 1.

Theorem 1 (Tails of $\text{PYP}(0, M, G_0)$). *Let $G(y)$ be the distribution of a $\text{DP}(M, G_0)$ process, with non-atomic G_0 . Then,*

$$\liminf_{y \rightarrow y_+} \frac{1 - G(y)}{g_s\{1 - G_0(y)\}} = \begin{cases} 0, & \text{if } s < 1, \\ \infty, & \text{if } s > 1, \end{cases} \quad a.s.,$$

$$\limsup_{y \rightarrow y_+} \frac{1 - G(y)}{h_r\{1 - G_0(y)\}} = \begin{cases} 0, & \text{if } r > 1, \\ \infty, & \text{if } r \leq 1, \end{cases} \quad a.s.,$$

with $g_s(t) = \exp\{-s \log |\log t|/t\}$ and $h_r(t) = \exp\{-1/(t |\log t|^r)\}$ for $0 < t < 1$.

Proof. See Doss and Sellke (1982) or Ghosal and Van der Vaart (2015, Theorem 4.22). \square

It follows from Theorem 1 that for large values of y , with probability one, we have the following lower and upper envelopes for the tail,

$$\exp \left[- \frac{s \log |\log M\{1 - G_0(y)\}|}{M\{1 - G_0(y)\}} \right] \leq 1 - G(y) \leq \exp \left[- \frac{1}{M\{1 - G_0(y)\} |\log M\{1 - G_0(y)\}|^r} \right], \quad (5)$$

for $s < 1$ and $r > 1$, where $G \sim \text{PYP}(0, M, G_0)$. Hence, the tails of the Dirichlet process are almost exponential, even if G_0 is heavy-tailed. Despite being one of the most popular Bayesian nonparametric priors, such deficiency of the DP rules out its use when the goal is to model heavy tails, extreme values, and risk. As shown next, what happens with the stable law process is substantially different as its tails are close to those of the baseline.

Theorem 2 (Tails of $\text{PYP}(D, 0, G_0)$). *Let $G(y)$ be the distribution of an $\text{SP}(D, G_0)$ process, with non-atomic G_0 . Then,*

$$\liminf_{y \rightarrow y_+} \frac{1 - G(y)}{l\{1 - G_0(y)\}} = D(1 - D)^{(1-D)/D}/S(1) \quad a.s.,$$

$$\limsup_{y \rightarrow y_+} \frac{1 - G(y)}{u_r\{1 - G_0(y)\}} = \begin{cases} 0, & r > 1, \\ \infty, & r \leq 1, \end{cases} \quad a.s.,$$

with $l(t) = t^{1/D} \{\log |\log t|\}^{1-1/D}$ for $0 < t < e^{-1}$, and $u_r(t) = t^{1/D} |\log t|^{r/D}$ for $0 < t < e^{-r}$.

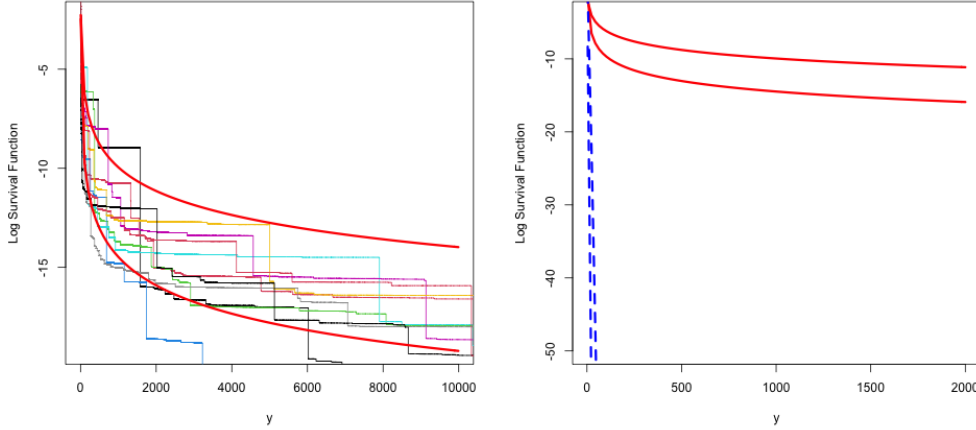


Figure 1: Asymptotic envelopes for Example 3. Left: Asymptotic envelopes that follow from Theorem 2 along with random trajectories of the log survival functions from a $\text{PYP}(0.5, 0, G_0)$. Right: The same envelopes for log survival function of $\text{PYP}(0.5, 0, G_0)$ (solid) against those of $\text{PYP}(0, 1, G_0)$ (dashed); G_0 is the standard unit Pareto distribution.

Theorem 2 warrants some remarks. The upshot of Theorem 2 is that the tails of a random distribution following a $\text{PYP}(D, 0, G_0)$ are almost as heavy as those of the centering, G_0 . Indeed, a consequence of Theorem 2 is that for large values of y , with probability one,

$$1 - G_0(y)^{\frac{1}{D}} [\log |\log \{1 - G_0(y)\}|]^{1-1/D} \leq 1 - G(y) \leq \{1 - G_0(y)\}^{1/D} |\log \{1 - G_0(y)\}|^{r/D}, \quad (6)$$

for $r > 1$ and $1 - G_0(y) < e^{-r}$. Numerical illustrations of the asymptotic envelopes in (6) are presented in Figure 1, and further examples are included in the supporting information. Another implication of Theorem 2 is that if the tail of the centering distribution of $\text{PYP}(D, 0, G_0)$ is heavy-tailed, then so will be that of the corresponding process, though with a lighter tail.

Theorem 3 (Stability of the heavy-tail property). *If $G \sim \text{PYP}(D, 0, G_0)$, with $D \in (0, 1)$, and G_0 is non-atomic and has a regularly varying tail, with tail index $\alpha_0 \equiv \alpha(G_0) > 0$, then G has a regularly varying tail, with tail index $\alpha(G) = \alpha(G_0)/D$, almost surely.*

Next, we compare Theorems 1 and 2 in a parametric example.

Example 3 (Pareto centering distribution—DP versus SP). Suppose first that $G \sim \text{DP}(M, G_0)$, where G_0 is a standard Pareto distribution, that is, $1 - G_0(y) = 1/y$, for $y > 1$. Then (5) yields

$$\exp[-sy/M \log |\log(M/y)|] \leq 1 - G(y) \leq \exp[-y/\{M |\log(M/y)|^r\}], \quad (7)$$

for $s < 1$ and $r > 1$, and hence the tails of $G \sim \text{DP}(M, G_0)$ are almost exponential, despite the fact that G_0 is heavy-tailed. Indeed, as shown in the supporting information (Section 2), the two bounds in (7) are in the Gumbel maximum domain of attraction, although G_0 is in the Fréchet maximum domain of attraction. Suppose now that $G \sim \text{SP}(D, G_0)$. Then,

$$y^{-1/D} \{\log |\log y^{-1}|\}^{1-1/D} \leq 1 - G(y) \leq y^{-1/D} |\log y^{-1}|^{r/D}.$$

It follows from Theorem 3 that $1 - G$ is regularly varying at infinity with tail index $1/D$. Figure 1 illustrates that, as predicted by Theorem 2, the trajectories of the stable process follow the asymptotic envelopes in (3); in addition, the same figure illustrates that the envelopes of the DP in (5) fall abruptly in comparison with those of the SP.

2.2 Heavy-tailed Pitman–Yor mixture models

Empowered by the main findings from Section 2.1, this section shows that two classes of heavy-tailed Pitman–Yor mixture models can be devised, and it discusses the relative merits of each option. Below, we focus on univariate mixtures; comments on multivariate as well as conditional extensions are given in Section 3.

Heavy-tailed PYP scale mixtures: The first class of mixture models to be considered will be of the type,

$$\begin{cases} f(y) = \int_0^\infty K_\sigma(y; \eta_\sigma) dG(\sigma), \\ G \sim \text{PYP}(D, 0, G_0(\sigma)), \\ 1 - G_0(\sigma) = \frac{\mathcal{L}(\sigma)}{\sigma^{\alpha_0}}, \end{cases} \quad (8)$$

with $y \in \mathbb{R}$ and $\alpha_0 \equiv \alpha(G_0) > 0$. Here, $K_\sigma(\cdot) = K(\cdot/\sigma; \eta_\sigma)/\sigma$ with K being a kernel, $\sigma > 0$ is a scale parameter, η_σ denotes additional parameters (possibly related with σ), and \mathcal{L} is a slowly varying function, that is, $\mathcal{L}(yt)/\mathcal{L}(y) \rightarrow 1$ as $y \rightarrow \infty$ for any $t > 0$.

Heavy-tailed PYP shape mixtures: The second class of mixture models to be considered is

$$\begin{cases} f(y) = \int_0^\infty \mathbb{k}(y; \alpha, \eta_\alpha) dG(\alpha), \\ G \sim \text{PYP}(D, M, G_0(\alpha)), \\ 1 - \mathbb{K}(y; \alpha, \eta_\alpha) = \frac{\mathcal{L}(y)}{y^\alpha}, \end{cases} \quad (9)$$

with $y \in \mathbb{R}$ and $\alpha \geq 0$. Here, \mathbb{k} is an Pareto-type kernel with distribution function \mathbb{K} , η_α denotes additional parameters (possibly related with α), and \mathcal{L} is a slowly varying function.

The following theorem implies that PYP mixture models in (8) and (9) are indeed heavy-tailed, and in addition it shows how their tail indices relate with that of the centering. Here and below $(a)_+ = \max(a, 0)$ denotes the positive part function.

Theorem 4 (Heavy-tailed PYP mixtures). *The following results hold for F the distribution function of f in (8) and (9):*

- a) *If (8) holds, with $U \sim K_\sigma(\cdot; \eta_\sigma)$, $E(U_+^{\alpha_0}) < \infty$, $P(U_+ > \sigma) = o\{1 - G_0(\sigma)\}^{1/D}$ and $\liminf_{\sigma \rightarrow \infty} \mathcal{L}(\sigma) > 0$, then the tail of f is regularly varying with tail index $\alpha(F) = \alpha_0/D$, almost surely.*
- b) *If (9) holds, then the tail of f is regularly varying with tail index $\alpha(F) = \inf\{\alpha : G_0(\alpha) > 0\}$, for any $G \sim \text{PYP}(D, M, G_0(\alpha))$, almost surely.*

Some comments on Theorem 4 are in order:

- Theorem 4 a) shows that if the centering of the stable process is heavy-tailed, and if the tail of the kernel is not heavier than that of the mixing, then f in (8) is heavy-tailed—with the same tail index as that of the mixing; that is, $\alpha(F) = \alpha(G) = \alpha_0/D$ with probability one, where $\alpha_0 = \alpha(G_0)$. Interestingly, this result offers a partial answer to an insightful open problem raised by Li et al. (2019, Theorem 3.5) on the range of $\alpha(F)$ under a polynomial decay of G_0 . Indeed, Theorem 4 a) illustrates that under a polynomial decay of G_0 , it holds that $\alpha(F) = \alpha_0/D$ differs from 0 and ∞ , almost surely, and thus $\alpha(F)$ for (8) does not concentrate on a singleton when assigned hyperpriors on D an α_0 . The range of $\alpha(F)$ can be the positive real line, provided that $\mathbf{p}(D) > 0$ or $\mathbf{p}(\alpha_0) > 0$, for all $0 < D < 1$ and $\alpha_0 > 0$ with $\mathbf{p}(\alpha_0)$ and $\mathbf{p}(D)$ denoting the prior densities of α_0 and D , respectively.

Distribution	Kernel (\mathbb{k})	Slowly varying function (\mathcal{L})	Tail index ($\alpha_{\mathbb{k}}$)
Burr	$\propto y^{c-1}/(1+y^c)^{a+1}$	$\propto (y^{-c} + 1)^{-(a+1)}$	ca
F	$\propto y^{a/2-1}(a+by)^{-(a+b)/2}$	$\propto (a/y + b)^{-(a+b)/2}$	$b/2$
Generalized Pareto	$\propto (1 - ay/\sigma)^{1/a-1}$	$\propto (1/y - k/\sigma)^{1/a-1}$	$-1/a$
Pareto	$\propto y^{-(a+1)}$	$\propto 1$	a
Student- t	$\propto (1 + y^2/a)^{-(a+1)/2}$	$\propto (1/y^2 + 1/a)^{-(a+1)/2}$	a

Table 1: Instances of Pareto-type kernels \mathbb{k} following (9)

- Theorem 4 b) is a folklore result that formalizes the idea that infinite shape mixtures of heavy-tailed kernels are themselves heavy-tailed, with tail index equal to that of the heaviest component (i.e., equal to the left endpoint of the centering in the case of (9)). As it is evident from the proof, the argument holds more generally for any random distribution G and not just for Pitman–Yor processes.

For simplification, throughout we refer to (8) as scale mixtures but as it will be shown below (8) also includes scale–shape mixtures of light-tailed kernels. Next, we present instances of the specifications in (8) and (9), that showcase the generality of the latter and how they relate with some mainstream approaches.

Example 4 (PYP scale mixtures with an Erlang kernel). As an example of (8) consider

$$f(y) = \sum_{h=1}^{\infty} \pi_h \text{Er}(y; a, \sigma_h), \quad (10)$$

where $\text{Er}(y; a, \sigma_h)$ is the density of the Erlang distribution with shape $a \in \mathbb{N}$ and scale $\sigma_h > 0$, and $\pi_h = V_h \prod_{k < h} (1 - V_k)$ with $V_h \stackrel{\text{ind}}{\sim} \text{Beta}(1 - D, M + hD)$, for $h \in \mathbb{N}$. In the notation of (8), with $K(y; \eta_\sigma) = \text{Er}(y; a, 1)$ and $\eta_\sigma = a$. For this kernel, the infinite mixture in (8) shows a connection with the phase-type scale mixtures of Bladt and Rojas-Nandayapa (2018). Two key differences are that: *i*) since the mixing in (8) is over a Pitman–Yor process inference can be conducted by standard Bayesian nonparametric samplers, whereas fitting phase-type scale mixtures is far from straightforward; *ii*) Theorem 4 a) allows for a general kernel with a lighter tail than that of the mixing, whereas Bladt and Rojas-Nandayapa (2018) consider phase-type kernels. Another version of (8), along the same lines as (10), which we have found to perform well in practice is the following scale–shape mixture of PYP,

$$f(y) = \sum_{h=1}^{\infty} \pi_h \text{Er}(y; \lceil \sigma_h \rceil, \sigma_h/\lambda), \quad (11)$$

where $\lceil \cdot \rceil$ is the ceiling function, and $K(y; \eta_\sigma) = \text{Er}(y; \lceil \sigma \rceil, 1/\lambda)$ with $\eta_\sigma = (\lceil \sigma \rceil, 1/\lambda)^\top$ in the notation of (8). We will revisit (11) later in the paper.

Example 5 (PYP shape mixtures with a Pareto-type kernel). Since the Burr, F , and generalized Pareto distributions are particular cases of Pareto-type kernels (Table 1), the mixture model in (9) includes as particular cases infinite mixtures of such distributions with a PYP mixing. In addition, (9) also includes the Pareto kernel Dirichlet process mixtures of Tressou (2008).

There are some reasons for preferring the stable process scale mixtures in (8) over (9). In particular, scale mixtures of stable processes offer a more natural link between the tail of the centering and the

tail of F than (9). For example, if in (8) the centering is a Pareto Type II distribution over $(0, \infty)$ (i.e., $1 - G_0(\sigma) = (1 + \sigma)^{-\alpha_0}$) then $\alpha(F) = \alpha_0/D$, and hence both the centering and F are heavy-tailed. Yet, if the centering in (9) is a Pareto Type II distribution over $(0, \infty)$ (i.e., $1 - G_0(\alpha) = (1 + \alpha)^{-\beta}$), then $\alpha(F) = 0$ and hence while the centering is heavy-tailed, F is super-heavy tailed. Motivated by this, in the next sections, we will emphasize scale mixtures of stable processes.

3 CONSEQUENCES AND EXTENSIONS

3.1 Multivariate variants

We now discuss how Section 2.2 can be extended to define priors on the space of multivariate heavy-tailed distributions, that is, the class of joint distributions with heavy-tailed marginals. Our construction follows the principles in Sarabia Alegría et al. (2008, Section 3.1), and it entails assuming conditional independence among components along with a common parameter shared by all components. This yields the following multivariate versions of (8) and (9) for $\mathbf{y} \in \mathbb{R}^d$. First, extending (8) consider the following multivariate heavy-tailed stable process scale mixture model:

$$\begin{cases} f(\mathbf{y}) = \int_{\mathbb{R}_+^d} \prod_{k=1}^d K_{\sigma_k}(y_k; \eta_{\sigma_k}) dG(\boldsymbol{\sigma}), \\ G \sim \text{PYP}(D, 0, G_0(\boldsymbol{\sigma})), \\ 1 - G_{0,k}(\sigma) = \frac{\mathcal{L}_k(\sigma)}{\sigma^{\alpha_{0,k}}}, \end{cases} \quad (12)$$

where $\boldsymbol{\sigma} = (\sigma_1, \dots, \sigma_d) \in \mathbb{R}_+^d$, and $G_{0,k}(\sigma)$ is the k th marginal distribution of $G_0(\boldsymbol{\sigma})$, for $k = 1, \dots, d$. Second, extending (9), consider the following multivariate heavy-tailed PYP shape mixtures:

$$\begin{cases} f(\mathbf{y}) = \int_{\mathbb{R}_+^d} \prod_{k=1}^d \mathbb{K}(y_k; \alpha_k, \eta_{\alpha_k}) dG(\boldsymbol{\alpha}), \\ G \sim \text{PYP}(D, M, G_0(\boldsymbol{\alpha})), \\ 1 - \mathbb{K}(y; \alpha_k, \eta_{\alpha_k}) = \frac{\mathcal{L}_k(y)}{y^{\alpha_k}}, \end{cases} \quad (13)$$

where $\boldsymbol{\alpha} = (\alpha_1, \dots, \alpha_d) \in \mathbb{R}_+^d$, \mathcal{L}_k is a sequence of slowly varying functions, and $G_{0,k}(\alpha)$ will denote the k th marginal distribution of $G_0(\boldsymbol{\alpha})$, for $k = 1, \dots, d$.

Theorem 5 (Multivariate heavy-tailed PYP mixtures). *The following results hold for F_k the distribution function of the k th marginal distribution of f in (12) and (13):*

- a) *If (12) holds, with k th marginal such that, $U_k \sim K_{\sigma_k}(\cdot; \eta_{\sigma_k})$ satisfying $E(U_{k+}^{\alpha_{0,k}}) < \infty$, $P(U_{k+} > \sigma) = o\{1 - G_0(\sigma)\}^{1/D}$ and $\liminf_{\sigma \rightarrow \infty} \mathcal{L}(\sigma) > 0$, then the k th marginal of f has a regularly varying tail with tail index $\alpha(F_k) = \alpha_{0,k}/D$, almost surely for $k = 1, \dots, d$.*
- b) *If (13) holds, then the k th marginal of f has a regularly varying tail with tail index $\alpha(F_k) = \inf\{\alpha : G_{0,k}(\alpha) > 0\}$, for any $G \sim \text{PYP}(D, M, G_0(\boldsymbol{\alpha}))$, almost surely.*

The previous result naturally extends Theorem 4 to the multivariate setting.

Remark 1. Some comments on the multivariate heavy-tailed stable process scale mixtures in (12) are in order:

- A concrete instance of (12) that we have found to work well in practice is the following extension of Example 4,

$$f(\mathbf{y}) = \sum_{h=1}^{\infty} \pi_h \prod_{k=1}^d \text{Er}(y_k; \lceil \sigma_{k,h} \rceil, \sigma_{k,h}/\lambda), \quad (14)$$

where once more $\text{Er}(y; a, b)$ is the density of the univariate Erlang distribution and $\pi_h = V_h \prod_{k < h} (1 - V_k)$ with $V_h \stackrel{\text{ind}}{\sim} \text{Beta}(1 - D, hD)$, for $h \in \mathbb{N}$.

- The specification in (12) requires that the centering is itself a multivariate heavy-tailed distribution. These can be easily constructed from copulas (Nelsen, 2006), and we recommend opting for Pareto Type II margins; that is, for $k = 1, \dots, d$,

$$1 - G_{0,k}(\sigma) = \left(1 + \frac{\sigma}{\beta}\right)^{-\alpha_{0,k}}, \quad (15)$$

with $\sigma \geq 0$, $\alpha_k > 0$, and $\beta > 0$. Such margins for the centering are convenient since they lead to a closed-form posterior of the extreme value index, as can be seen from the supporting information (Section 2).

- To complete (12) we recommend a Jeffrey's prior on the tail index $\mathbf{p}(\alpha_{0,k}) \propto 1/\alpha_{0,k}$ and a Beta prior on the discount parameter, $D \sim \text{Beta}(a_D, b_D)$. Finally, one may set a prior on the remainder parameters of the kernel, and for instance in the Erlang kernel example in (14), we will opt for $\lambda \sim \text{Gamma}(a_\lambda, b_\lambda)$. This implies a prior for the tail index α_0/D , with infinite expectation. Alternatively, with a proper prior on α_0 , e.g. $\alpha_0 \sim \Gamma(a_{\alpha_0}, b_{\alpha_0})$, the induced prior on the tail index would have prior expectation $E(\alpha_0)E(1/D) = \{a_{\alpha_0}(a_D + b_D - 1)\} / \{b_{\alpha_0}(a_D - 1)\}$.

3.2 Modeling conditional joint densities

We now show how to extend the proposed models so to include the effect of covariates by using a single atoms dependent Pitman–Yor process extending the principles from Barrientos et al. (2012, Definition 3) and Quintana et al. (2022, Section 2.3). For conciseness, we focus on multivariate heavy-tailed PYP scale mixtures in (12), but the principles discussed below can be easily adapted for the multivariate shape mixtures from Section 3.1 as well as to the univariate methods from Section 2. Consider the following predictor-dependent model,

$$f(\mathbf{y} \mid \mathbf{x}) = \int_{\mathbb{R}_+^d} \prod_{k=1}^d K_{\sigma_k}(y_k; \eta_{\sigma_k}) dG_{\mathbf{x}}(\boldsymbol{\sigma}), \quad (16)$$

where $\mathbf{y}, \boldsymbol{\sigma} \in \mathbb{R}^d$ and $\{G_{\mathbf{x}}\}$ is a family of random probability measures indexed by a covariate $\mathbf{x} \in \mathbb{R}^p$. Specifically, we consider the following dependent stable process

$$G_{\mathbf{x}} = \sum_{h=1}^{\infty} \pi_h(\mathbf{x}) \delta_{\boldsymbol{\sigma}_h}, \quad \boldsymbol{\sigma}_h \stackrel{\text{iid}}{\sim} G_0(\boldsymbol{\sigma}). \quad (17)$$

Here, the weights of the stick-breaking representation and the discount parameter D of the Pitman–Yor process are indexed over the covariate as follows, $\pi_h(\mathbf{x}) = V_h(\mathbf{x}) \prod_{k < h} \{1 - V_k(\mathbf{x})\}$, and

$$V_h(\mathbf{x}) \sim \text{Beta}(1 - D_h(\mathbf{x}), hD_h(\mathbf{x})), \quad D_h(\mathbf{x}) = \frac{e^{\mathbf{x}^T \boldsymbol{\beta}_h}}{1 + e^{\mathbf{x}^T \boldsymbol{\beta}_h}}, \quad (18)$$

where β_h is a parameter in \mathbb{R}^p . Clearly, since (17) is a PYP for every \mathbf{x} , Theorem 5 a) implies that the joint density mixture model in (16) yields a multivariate heavy-tailed distribution, for every \mathbf{x} . The model is completed with a prior distribution for β_h , given by $\beta_h \stackrel{\text{iid}}{\sim} N_p(\mathbf{0}, s^2 \mathbf{I})$, for $h \in \mathbb{N}$. A specific embodiment of the approach discussed in this section, that will be revisited later in the paper, is the following extension of Example 4,

$$f(\mathbf{y} \mid \mathbf{x}) = \sum_{h=1}^{\infty} \pi_h(\mathbf{x}) \prod_{k=1}^d \text{Er}(y_k; \lceil \sigma_{k,h} \rceil, \sigma_{k,h}/\lambda), \quad (19)$$

where $\pi_h(\mathbf{x}) = V_h(\mathbf{x}) \prod_{k < h} \{1 - V_k(\mathbf{x})\}$, with $V_h(\mathbf{x}) \sim \text{Beta}(1 - D_h(\mathbf{x}), hD_h(\mathbf{x}))$, and $D_h(\mathbf{x}) = e^{\mathbf{x}^T \beta_h} / (1 + e^{\mathbf{x}^T \beta_h})$, for $h \in \mathbb{N}$.

4 SIMULATION STUDY

4.1 Simulation scenarios and preparations

This section describes the true data generating processes and the settings used over the Monte Carlo simulation study from Section 4.2.

Data generating processes: We consider one scenario for the univariate version of the model from Section 2.2, three scenarios for the multivariate version from Section 3.1, and three scenarios for the multivariate conditional version from Section 3.2. The univariate scenario is a standard unit Pareto distribution with tail function $1 - F(y) = 1/y$, for $y > 1$, and its main aim will be to highlight that for heavy-tailed data, stable process mixing leads to much better fits at the tails than Dirichlet process mixing. Beyond the univariate scenario, we also considered bivariate and conditional scenarios that contemplate different dependence levels and complexities of the marginals. Table 2 summarizes the bivariate and conditional scenarios, which are marginally characterized by

$$\begin{cases} f_k(y) = w f_{\text{LG}}\{y \mid a_1, b_1\} + (1 - w) f_{\text{LG}}\{y \mid a_2, b_2\}, \\ f_k(y \mid x) = w f_{\text{LG}}\{y \mid a_1(x), b_1(x)\} + (1 - w) f_{\text{LG}}\{y \mid a_2(x), b_2(x)\}, \end{cases} \quad (20)$$

for $k = 1, 2$, where $f_{\text{LG}}(y; a, b) = b^a \log(y)^{a-1} y^{-(b+1)} / \Gamma(a)$ is the density of a log-Gamma distribution with shape $a > 0$ and rate $b > 0$; parenthetically, we note that the log-Gamma distribution is in the Fréchet domain of attraction with tail index b (Beirlant et al., 2004, Table 2.1).

The dependence is modeled via a Gumbel copula, so that data for the bivariate and conditional scenarios are respectively simulated from

$$\begin{cases} F(y_1, y_2) = C_\theta\{F_1(y_1), F_2(y_2)\}, \\ F(y_1, y_2 \mid x) = C_\theta\{F_1(y_1 \mid x), F_2(y_2 \mid x)\}. \end{cases} \quad (21)$$

Here, $C_\theta(u, v) = \exp[-\{(-\log u)^\theta + (-\log v)^\theta\}^{1/\theta}]$, for $(u, v) \in (0, 1)^2$, whereas $\theta \geq 1$ is the parameter controlling dependence, and F_1 and F_2 are the distribution functions of f_1 and f_2 . For all scenarios, we have simulated $n = 1\,000$ observations, and for the conditional scenarios covariates were drawn from a standard uniform distribution.

Scenario	Marginal (f_1)	Marginal (f_2)	Copula (θ)
Bivariate 1	$a_1 = a_2 = 5; w = 1$	$a_1 = a_2 = 5; w = 1$	3
2	$a_1 = a_2 = 5; w = 1$	$a_1 = a_2 = 5; w = 1$	1
3	$a_1 = 13; b_1 = 7;$ $a_2 = 10; b_2 = 8; w = .4$	$a_1 = 8; b_1 = 7;$ $a_2 = 15; b_2 = 8; w = .4$	1
Conditional 1	$a_1 = 1 + 4x; a_2 = 3; w = 1$	$a_1 = 1 + 4x; a_2 = 3; w = 1$	1
2	$a_1 = 1 + 4x; a_2 = 3; w = 1$	$a_1 = 1 + 4x; a_2 = 3; w = 1$	3
3	$a_1 = 11 + 5x; b_1 = 8 + 5x;$ $a_2 = b_2 = 7; w = .4$	$a_1 = 6 + 5x; b_1 = 12 + 5x;$ $a_2 = b_2 = 8; w = .4$	1

Table 2: Bivariate and Conditional Simulation Scenarios. The marginals are mixtures of log-Gamma distributions as in (20), and dependence is set by a Gumbel copula with parameter θ

MCMC and model specification: All models were fitted using the slice sampler (Walker, 2007) available from the supporting information (Section 2). We considered a burn-in period of 5 000 iterations, and after that scanned 5 000 samples from the posterior targets of interest. For the univariate scenario we fitted a stable process scale mixture with an uninformative Gamma prior and an Erlang kernel (i.e., (11) with prior $\lambda \sim \text{Gamma}(0.1, 0.1)$); for the bivariate and conditional scenarios we fitted stable process scale mixtures with an Erlang kernel based on Remark 1 and Equation (19), respectively. For the latter, a Gumbel copula was used for the centering, and empirical Bayes was used to set the hyperparameter for θ via maximum likelihood. For the conditional version of the model in the regression parameters in (18), we consider the prior $\beta_h \stackrel{\text{iid}}{\sim} N_p(\mathbf{0}, s^2 \mathbf{I})$, and set the hyperparameter to be $s^2 = 100$. For the hyperparameters of the marginals Pareto for the base measure, we set $\beta_k = 1$ and tail index $\alpha_{0,k} = 2$, for $k = 1, 2$, which implies that both margins are a priori heavy-tailed but have a finite expected value. Finally, we have assigned the prior $D \sim \text{Beta}(0.5, 0.5)$ to the discount parameter for all instances of the model. Keeping in mind space constraints, and the preference for stable process scale mixtures noted in Section 2.2, here we mainly concentrate on assessing the performance of the latter. The posterior inference algorithms available from the supporting information (Section 2) can however be used for fitting multivariate as well as conditional heavy-tailed PYP shape mixtures, and some instances of the latter are available from the `pitvOR` package.

One-shot experiments: One-shot experiments for the bivariate and conditional scenarios are presented in the supporting information (Section 3). All in all, the resulting fits suggest that the proposed methods accurately recover the true distribution for all scenarios being examined. Such findings should of course be regarded as tentative, as they are the outcome of a single run experiment and will be subject to the scrutiny of the Monte Carlo simulation study in the next section.

4.2 Monte carlo simulation study

We now report the main findings of a Monte Carlo simulation study. For each scenario from Section 4.1, we simulated 100 data sets each containing $n = 1\,000$ observations. All models have been fitted using stable process scale mixture models with the same specifications and MCMC settings as described in Section 4.1. We start with the univariate unit Pareto scenario, which will reinforce our preference for stable process scale mixture models.

In Figure 2 we present the posterior Monte Carlo means of the log-survival estimates for the tail of the univariate scenario and compare it with the corresponding Monte Carlo mean for a Dirichlet

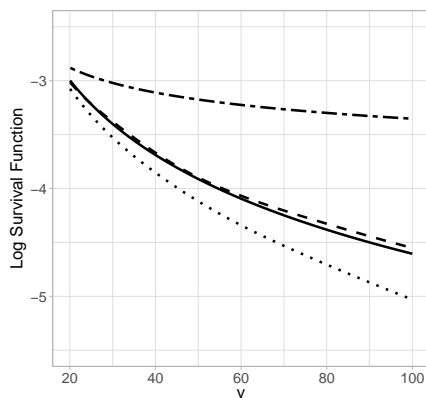


Figure 2: Mean of the Monte Carlo fits (dashed line) for the log-survival function for the univariate scenario obtained using the stable process scale mixture model from Section 2.2, from the 95% to the 99% quantile, plotted against the true (solid line). The dotted line shows the Monte Carlo mean of the fits from a DPM with the same Erlang kernel, whereas the dashed–dotted line shows the Monte Carlo mean of the fits from a DPM with a Pareto kernel and a Gamma centering distribution.

process mixture based on the same kernel. As can be seen from Figure 2, stable process mixing accurately estimates the tail, whereas Dirichlet process mixing markedly underestimates it; this numerical evidence showcases that the proposed stable process scale mixtures are a natural option for modeling risk and extremes in a heavy-tailed framework. Such numerical performance of the proposed methods finding is not surprising in light of Theorem 4 a); the performance over the bulk (not shown) is comparable for both forms of mixing. Interestingly, Figure 2 also reveals that the Monte Carlo mean based on fitting Dirichlet process mixture with a Pareto kernel and a Gamma centering distribution overestimates the tail of the distribution. Such numerical finding is not surprising, keeping in mind Theorem 4 b), given that the left endpoint of the Gamma centering distribution function is 0 and hence the resulting mixture is super heavy-tailed (i.e. $\alpha(F) = 0$). Next, we move to the bivariate and conditional scenarios from Section 4.1. Figure 3 shows 100 posterior estimated contours for the three bivariate scenarios. As it can be seen from the latter figure, the proposed stable process scale mixture model can capture the true contours over different levels of dependence (Scenarios 1–2) and even with challenging marginals such as mixtures (Scenario 3). The results for the conditional scenarios are presented in the supporting information (Section 3) and also suggest an overall good performance of the proposed methods.

5 APPLICATION TO HEAVY-TAILED BRAIN DATA

5.1 Applied context and data description

We now showcase the application of the proposed methods to a neuroscience case study. Brain rhythm signals are key for understanding how the human brain works; loosely speaking, they consist of patterns of neuronal activity that are believed to be linked with certain behaviors, arousal intensity, and sleep states (Frank, 2009). These signals are typically measured using an electroencephalogram (EEG), which records electrical activity in the brain via electrodes attached to the scalp. An EEG

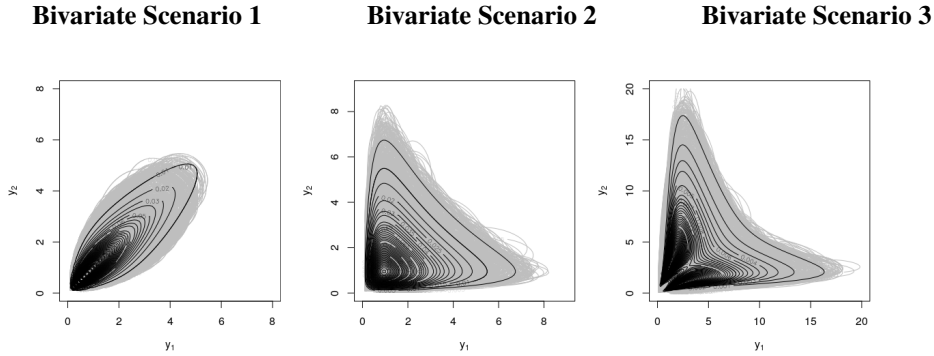


Figure 3: Monte Carlo Simulation for the Bivariate Scenarios 1–3: Contours of the joint density estimates (gray) obtained with proposed stable process scale mixture model from Section 3.1, for the 100 simulated data sets, plotted against the true (black).

signal tracks the activity of billions of neurons, and such signals cover a broad spectrum of frequency bands. Say, the alpha band typically refers to 8–13Hz, while beta refers to 13–20Hz; for a primer on brain rhythms and EEG signals, see for instance Buzsaki (2006) and Ombao et al. (2016, Ch. 7). Alpha and beta rhythms are believed to be heavy-tailed (e.g. Roberts et al., 2015), and hence the main goal of our analysis will be to learn about the marginal and joint distribution of these heavy-tailed oscillations, given a variety of stimuli to be described below. In the supporting information (Section 4), we report evidence supporting the claim that in line with Roberts et al. (2015) our alpha and beta brainwave data are indeed heavy-tailed. We assess this by learning from data about the so-called extreme value index of a generalized Pareto distribution—which is known to be positive for heavy-tailed data (Coles, 2001, Section 4). The data to be analyzed are available from the R package `pityoR`, and were gathered from a UC Berkeley study that involved 30 participants who were subject to several audio-visual activities and stimuli, namely: *mathematics*, *relaxation*, *music*, *color*, *video* as well as *relax and think*.

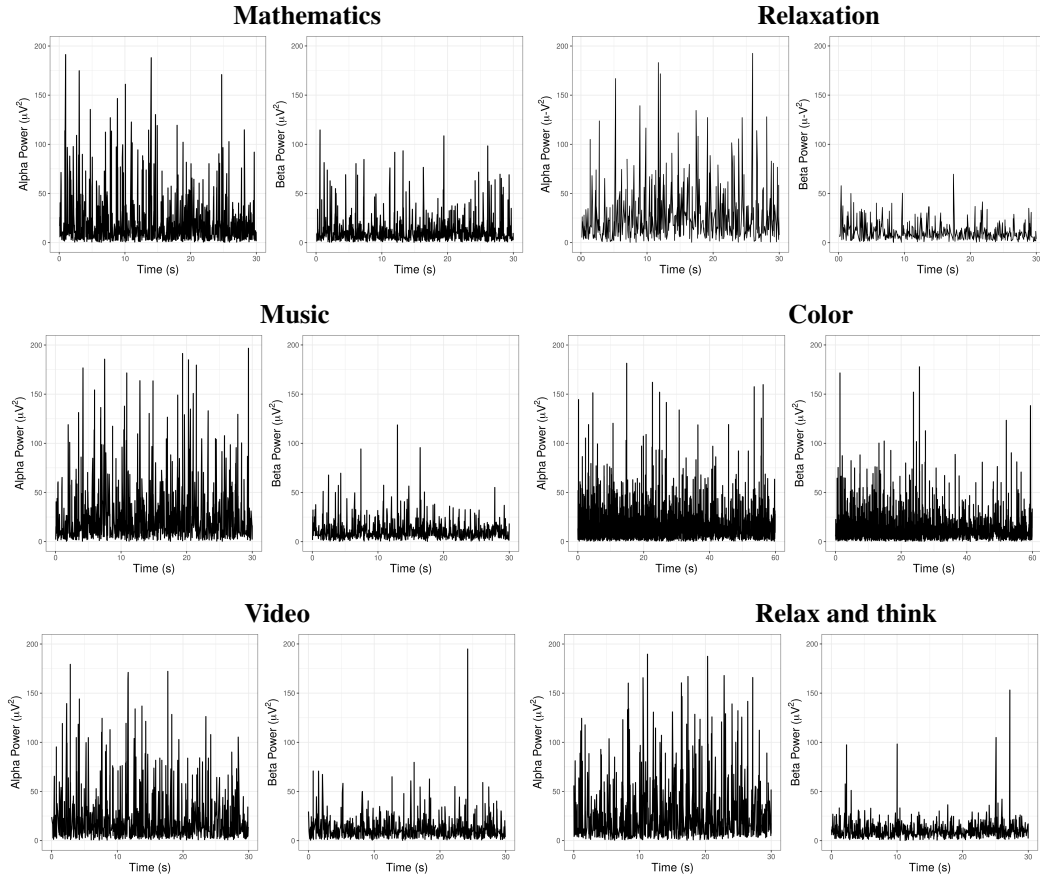


Figure 4: Spectral power (μV^2) of alpha and beta brainwave data plotted against time in seconds (s).

Figure 4 shows the spectral power in (micro)-Volts squared (μV^2) for alpha and beta waves for all participants; roughly speaking, higher peaks indicate higher neural activity at a certain point in time on a frequency band of interest. The Ljung–Box test results reported in the supporting information (Section 4) suggest that the recorded trajectories of spectral power can be regarded as independent over time across all stimuli. Figure 4 illustrates some aspects of alpha and beta bands that help to build intuition on their signatures for the different stimuli. For instance, when the stimulus is *mathematics* we can notice high activity for both alpha and beta waves, similar behavior to watching a *video* or finding the *color*—all these being tasks that relate to immediate attention. And indeed, it has been suggested that alpha bands tend to be associated with ‘attention’ as well as with ‘information processing’ (Klimesch, 2012). Interestingly, the patterns of alpha and beta waves for both *mathematics* and *music* are reasonably similar—which might not be surprising in light of what has been claimed elsewhere (e.g., Boettcher et al., 1994, and references therein). Whether that similarity of *mathematics* and *music* also holds for the *joint* distribution of alpha and beta waves is something to be examined below in Section 5.3. Next, we learn from the heavy-tailed brainwave data discussed above using the methods proposed in Sections 2–3. Except where mentioned otherwise, all fits have been conducted using the same model specifications and MCMC settings as in Section 4.

5.2 Marginal brainwave analysis

Figure 5 shows the marginal density estimates of alpha and beta power pooling all subjects for each stimulus that were obtained using the proposed stable process scale mixture model from Section 2.2. Specifically, the fits from Figure 5 were obtained using the specification in (11) along with an uninformative Gamma prior and an Erlang kernel. To assess the quality of the obtained fits, we depict in Figure 5 q-q boxplots (Rodu and Kafadar, 2022) of random quantile residuals (Dunn and Smyth, 1996).

The obtained q-q boxplots provide evidence that the stable process scale mixture adjusts well both the bulk and the right tail of the data. We have also compared the fitted stable process scale mixture model against the DP shape mixtures in (9) with a Pareto kernel and a Gamma centering distribution. In line with the findings from the univariate scenario of the simulation study in Section 4.2, we again found evidence in favor of a far more sensible behavior of the stable process scale mixture in comparison with the shape mixture of heavy-tailed kernels. The comparison of the q-q boxplots in Figure 5—for the stable process scale mixture—against those available from the supporting information (Section 4)—for the DP shape mixture of Pareto kernels—clearly indicates a better performance of the former over the latter over both the left and right tails.

5.3 Stimulus-specific joint brainwave analysis

While Section 5.2 offered a one-dimensional snapshot across different stimuli, we now apply the proposed methods so to learn about the joint distribution of the power of brainwaves on alpha and frequency bands, conditional on the activities and stimuli discussed in Section 5.1. To put it differently, we now apply the multivariate regression framework from Sections 3.1–3.2 so to learn about the conditional dependence structure governing alpha and beta rhythms, and to borrow strength across stimuli, rather than just fitting each density individually as in Section 5.2.

Figure 6 shows the contours of the fitted conditional joint densities, given the stimulus under analysis, and it sheds light on the dynamics governing the joint behavior of the alpha and beta brain rhythms. First, the joint densities for some stimuli look similar—such as, for example, *music* and *relax and think*—which suggests a similar joint behavior of the rhythms of alpha and beta bands for these stimuli. Second, *mathematics* and *music*—which looked similar just by examining the raw data in Figure 4 and the marginal fits in Figure 4—have a clearly different dependence structure as can be seen from Figure 6. In other words, while marginally the alpha- and beta-band oscillations for *mathematics* and *music* do look similar, their ‘synchronization’ or joint behavior looks markedly different.

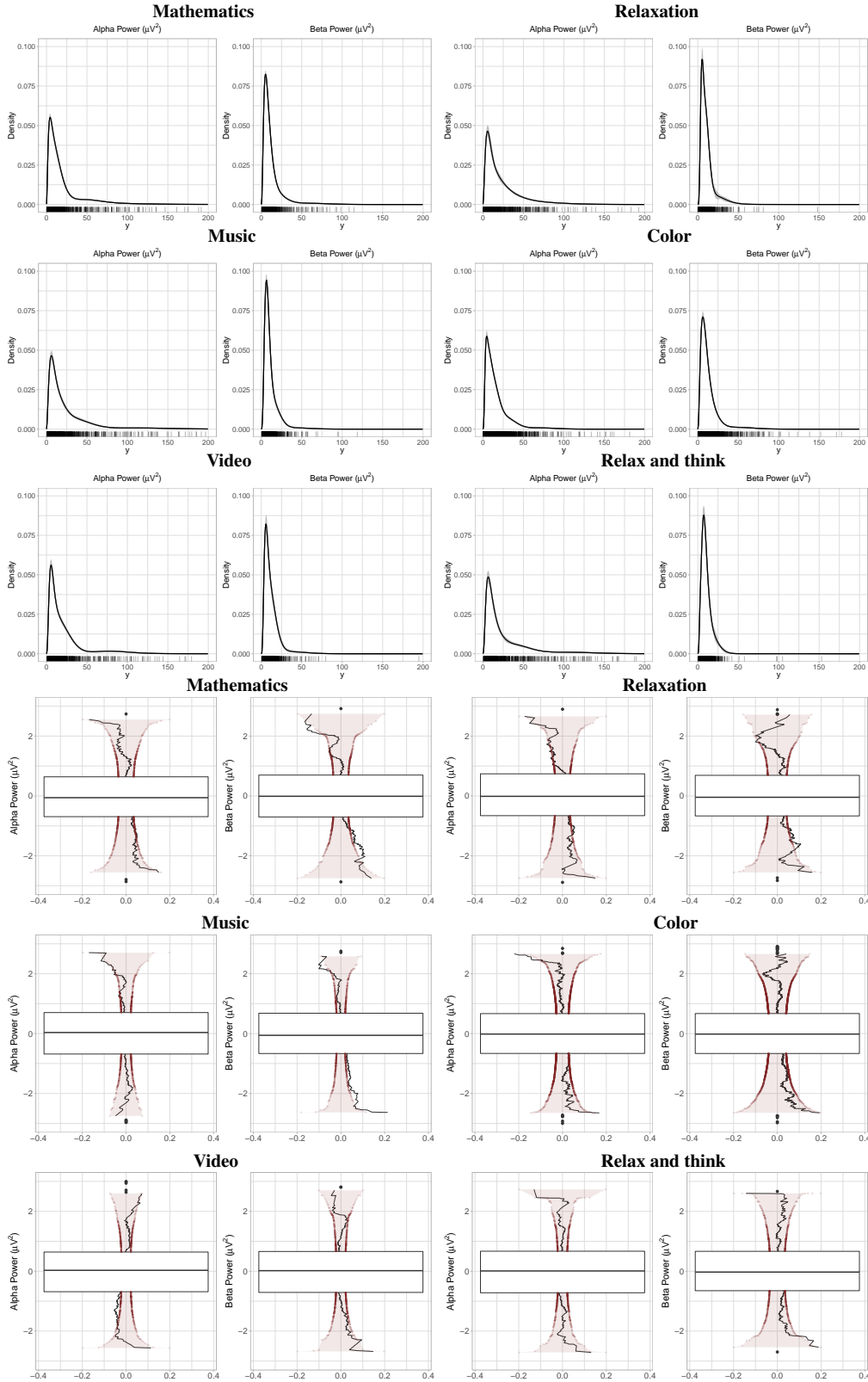


Figure 5: Top: Marginal density estimates of alpha and beta power for each stimulus, obtained with proposed stable process scale mixture model from Section 2.2, along with 95% credible bands. Bottom: Corresponding q-q boxplot of randomized quantile residuals.

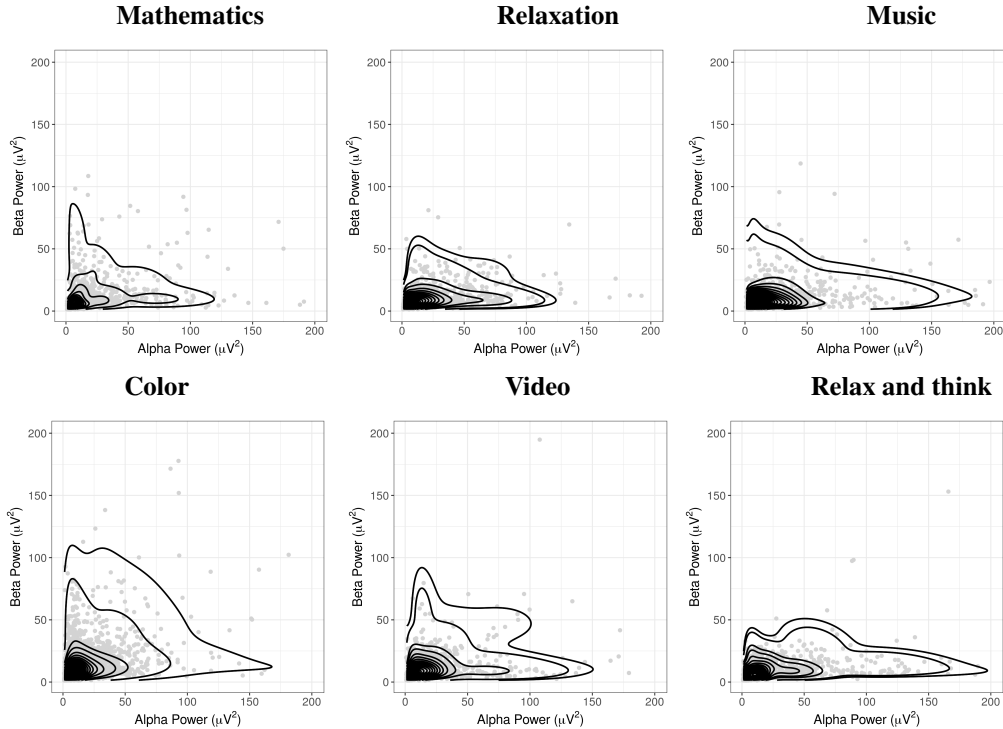


Figure 6: Contours of the posterior conditional joint density estimate of alpha and beta power for each specific stimulus along with raw data; the fit was obtained using the stable process scale mixture from Section 3.2.

6 CONCLUDING REMARKS

This paper studied the tails of some prominent Pitman–Yor processes, and it has shown in particular that the tail of the stable law process is tantamount to that of the baseline. This result is in clear contrast to what is known to hold for the DP, whose tails are exponentially much thinner than those of the centering; in addition, we have also derived for the first time envelopes on which the tail of the stable process must lie. We then devised two classes of heavy-tailed Pitman–Yor mixture models, along with their extensions to a multivariate heavy-tailed setting—as well as to a regression framework. Equipped with the above-mentioned characterization of the tails of the PYP, we have shown that not all heavy-tailed Pitman–Yor process mixture models are alike. To put it differently, our theoretical and numerical analyses pinpoint a clear preference for stable process scale mixtures over shape mixtures of heavy-tailed kernels. Particularly, we have shown that shape mixtures of Pareto-type kernels can be super heavy-tailed even though the centering is ‘only’ heavy-tailed; this implies that a naïve application of the latter mixture models might lead to an overestimation of the mass at the tail—along with poor inferences at the bulk of the distribution. On the contrary, we have found stable process scale mixtures to obey natural properties—such as the stability of the heavy-tail from Theorem 3—and to perform well numerically in both the bulk as well as in the right tail. Keeping in mind the scope of our case study as well as space constraints, we have concentrated the numerical illustrations on the right tail as well as on kernels supported over the positive real line. Yet, we underscore that the theory and methodologies from Sections 2–3 hold more generally over the entire real line as well as for left tails. Finally, the fact that other statistical functionals, such

as tail indices, can be readily inferred from the proposed methods implies that, as a byproduct, the conditional version from Section 3 may be used as a tail index regression model in the same vein as Wang and Tsai (2009).

We close the paper with some final comments on open challenges for future analysis. It seems reasonable to conjecture that the tail of the PYP for the case $M > -D$ with $0 < D < 1$ might suffer from similar issues like that of the DP; the analysis of the latter case is however as non-trivial as those presented herein, and hence we leave it as an open problem for future research. As we have shown here, stable law processes obey the stability of the heavy-tail property, and it would be interesting to have a broader understanding on how large is the class of random probability measures obeying that property. While here the focus has been on the Pitman–Yor processes and on their mixtures, the potential for modeling heavy-tailed data of other classes of random measures—such as those of Ayed et al. (2019)—remains highly unexplored. Finally, by keeping in mind the importance of modeling rare but catastrophic events in a variety of fields—such as climatology, geology, insurance, risk analysis, and extreme value theory—the methodologies proposed herein may pave the way for further applications and developments at the interface between heavy-tails and Bayesian nonparametrics.

SUPPORTING INFORMATION

Additional supporting information contains further technical details and supporting numerical evidence along with the R package `pit_yor` that implements instances of the methods proposed herein as well as the dataset from Section 5.

APPENDIX

A TECHNICAL DETAILS AND AUXILIARY LEMMATA

In addition to the auxiliary results below, we first recall a basic fact on subordinators that will be handy for the proof of Theorem 2. If $S(t)$ is a subordinator, then $S(t+h) - S(t)$ has the same distribution as $S(h)$, for every $t, h \geq 0$ (Bertoin, 1999, p. 5). This implies that $\{S(1) - S(t)\}_{t \in [0,1]}$ is equal in distribution to $\{S(1-t)\}_{t \in [0,1]}$, and hence the following subordinator representation holds for the tail of $G \sim \text{PYP}(\sigma, 0, G_0)$:

$$1 - G(y) \stackrel{(2)}{=} 1 - \frac{S\{G_0(y)\}}{S(1)} = \frac{S(1) - S\{G_0(y)\}}{S(1)} \stackrel{d}{=} \frac{S\{1 - G_0(y)\}}{S(1)}. \quad (22)$$

Lemma 1 gathers two well-known results on lower and upper envelopes of stochastic processes over the short-run which can be found in Bertoin (1999, Theorem 11) and Sato (1999, Proposition 47.16). Lemma 2 is a well-known result in regular variation Embrechts et al. (e.g. 1997, Theorem A.33) and for the extended Breiman’s lemma see Denisov and Zwart (2007, Proposition 2.1).

Lemma 1. *The following results hold:*

a) *If $\{S(t) : t \geq 0\}$ is a subordinator with Laplace exponent $\Phi \in \text{RV}_D$, with $D \in (0, 1)$, then*

$$\liminf_{t \rightarrow 0^+} |S(t)|/l(t) = D(1-D)^{(1-D)/D}, \quad a.s.,$$

where $l(t) = \log |\log t| / \Phi^{-1}(t^{-1} \log |\log t|)$ for $0 < t < e^{-1}$, and Φ^{-1} is the inverse function of Φ .

b) Let $\{S(t)\}$ be a D -stable process on \mathbb{R} with $0 < D < 2$ and $\nu(0, \infty) > 0$. If $u(t)$ is a real-valued function that is positive, continuous, and increasing on some $(0, \delta)$, and for which $u(t)/\{t \log \log(1/t)\}^{1/2} \rightarrow 0$, as $t \rightarrow 0^+$, then

$$\limsup_{t \rightarrow 0^+} \frac{S(t)}{u(t)} = \begin{cases} 0, & \int_0^\delta u^{-D}(t) dt < \infty, \\ \infty, & \int_0^\delta u^{-D}(t) dt = \infty, \end{cases} \quad a.s.$$

Lemma 2 (Representation theorem). *If $h \in RV_\alpha$ for some $\alpha \in \mathbb{R}$, then*

$$h(y) = c(y) \exp \left\{ \int_z^y \frac{a(u)}{u} du \right\}, \quad y \geq z,$$

for some $z > 0$ with $c(y) \rightarrow c \in (0, \infty)$, $a(u) \rightarrow \alpha$ as $y \rightarrow \infty$. The converse also holds.

Lemma 3 (Extended Breiman's lemma). *Let X and Y be random variables and suppose X has a regularly varying tail, $P(X > x) = x^{-\alpha} \mathcal{L}(x)$, with tail index $\alpha \geq 0$, and $Y \geq 0$ with $E(Y^\alpha) < \infty$. Then, if*

$$\liminf_{x \rightarrow \infty} \mathcal{L}(x) > 0 \quad \text{and} \quad P(Y > x) = o\{P(X > x)\},$$

it follows that XY has regularly varying tail with tail index α .

A.1 Proofs of main results

Proof of Theorem 2: We start with the lower envelope. The Laplace exponent of a D stable process, $\Phi(\lambda) = \lambda^D$, is regularly varying at ∞ with index $D \in (0, 1)$, and note also that $\Phi^{-1}(y) = y^{1/D}$. Hence, Lemma 1 a) implies that

$$\liminf_{t \rightarrow 0^+} \frac{S(t)}{l(t)} = D(1-D)^{(1-D)/D}, \quad \text{with } l(t) = t^{1/D} \{\log |\log t|\}^{1-1/D}. \quad (23)$$

Combining (23) with the representation of the stable law process in Example 2 yields

$$\liminf_{G_0(y) \rightarrow 0^+} \frac{S\{G_0(y)\}/S(1)}{l\{G_0(y)\}} = \liminf_{G_0(y) \rightarrow 0^+} \frac{G(y)}{l\{G_0(y)\}} = D(1-D)^{(1-D)/D}/S(1).$$

Hence, (22) yields

$$\liminf_{G_0(y) \rightarrow 1^-} \frac{1 - G(y)}{u_r\{1 - G_0(y)\}} = D(1-D)^{(1-D)/D}/S(1),$$

from where the final result follows. Next, we focus on the upper envelope. Consider the following family of functions for $r > 0$,

$$u_r(t) = t^{1/D} |\log t|^{r/D} = t^{1/D} \{\log(1/t)\}^{r/D}, \quad t \in (0, e^{-r}), \quad (24)$$

where $D \in (0, 1)$. We start by checking if $u_r(t)$ verifies the assumptions of Lemma 1 b). It follows that $u_r(t)$ is positive and nondecreasing on $(0, \delta)$, with $\delta = e^{-r}$. Indeed,

$$\begin{aligned} \frac{d}{dt} \{u_r(t)\} &= D^{-1} t^{1/D-1} \{\log(1/t)\}^{r/D} + t^{1/D} r D^{-1} \{\log(1/t)\}^{r/D-1} (-1/t) \\ &= D^{-1} t^{1/D-1} \{\log(1/t)\}^{r/D} - t^{1/D-1} r D^{-1} \{\log(1/t)\}^{r/D-1} \\ &= D^{-1} t^{1/D-1} [\{\log(1/t)\}^{r/D} - r \{\log(1/t)\}^{r/D-1}] > 0, \quad t \in (0, \delta). \end{aligned} \quad (25)$$

Additionally, it follows that

$$\lim_{t \rightarrow 0^+} \frac{u_r(t)}{\{t \log \log(1/t)\}^{1/2}} = \lim_{t \rightarrow 0^+} \frac{t^{1/D} \{\log(1/t)\}^{r/D}}{\{t \log \log(1/t)\}^{1/2}} \quad (26)$$

$$= \lim_{t \rightarrow 0^+} t^{1/D-1/2} \times \lim_{t \rightarrow 0^+} \frac{\{\log(1/t)\}^{r/D}}{\{\log \log(1/t)\}^{1/2}} \rightarrow 0, \quad (27)$$

as $t \rightarrow 0^+$ given that $1/D - 1/2 > 0$ (recall that $D < 1$), and hence $u_r(t)$ obeys the assumptions of Lemma 1(2). Hence applying Lemma 1(2), with (24), in the representation of the stable law process from Example 2 yields

$$\lim_{G_0(t) \rightarrow 0^+} \sup_{G(t)} \frac{G(t)}{u_r\{G_0(t)\}} = \begin{cases} 0, & r > 1, \\ \infty, & 0 < r \leq 1, \end{cases} \quad \text{a.s.} \quad (28)$$

Finally, Equation (22) implies the final result.

Proof of Theorem 3: It follows from Theorem 2 that as $y \rightarrow y_+$, then

$$1 - G(y) = \{1 - G_0(y)\}^{\{1+o(1)\}/D}, \quad \text{a.s.} \quad (29)$$

By assumption, $1 - G_0 \in \text{RV}_{-\alpha_0}$ and hence it follows by the representation theorem that $1 - G_0(y) = c(y) \exp\{\int_z^y b(u)/u \, du\}$, for some $z > 0$ with $c(y) \rightarrow c \in (0, \infty)$, $a(u) \rightarrow -\alpha_0$ as $y \rightarrow \infty$. This combined with (29) yields that

$$1 - G(y) = \{1 - G_0(y)\}^{\{1+o(1)\}/D} = c^*(y) \exp\left\{\int_z^y \frac{a^*(u)}{u} \, du\right\}, \quad y \geq z,$$

for some $z > 0$, with

$$c^*(y) = \{c(y)\}^{\{1+o(1)\}/D} \rightarrow c^{1/D} \in (0, \infty), \quad a^*(u) = \left(\frac{1+o(1)}{D}\right)b(u) \rightarrow -\alpha_0/D,$$

as $y \rightarrow \infty$. The final result follows from the representation theorem. \square

Proof of Theorem 4

- a) Let $U \mid V = \sigma \sim K(\cdot; \eta_\sigma)$ and $V \sim G$, and consider the decomposition $U = U_+ - U_-$, where $U_+ = \max(U, 0)$ and $U_- = \max(-U, 0)$. Since the focus is on the right tail, we concentrate on U_+ , and note below that for $y > 0$ the scale mixture in (8) can be written as the density of the product of U_+ and V . In detail, it follows from Rohatgi's well-known result on the product of random variables (e.g. Glen et al., 2004), that

$$f_{U_+V}(y) = \int_0^\infty f_{U_+,V}\left(\sigma, \frac{y}{\sigma}\right) \frac{1}{\sigma} \, d\sigma. \quad (30)$$

Hence, combining the fact that $U_+ \mid V = \sigma \sim K(y; \eta_\sigma)I(y > 0) + P(U_+ = 0 \mid V = \sigma)I(y = 0)$ along with Bayes theorem implies that (30) can be rewritten as follows

$$\begin{aligned} f_{U_+V}(y) &= \int_0^\infty f_{U_+|V}\left(\frac{y}{\sigma}, \sigma\right) \frac{dG(\sigma)}{d\sigma} \frac{1}{\sigma} \, d\sigma \\ &= \int_0^\infty K\left(\frac{y}{\sigma}; \eta_\sigma\right) \frac{1}{\sigma} \, dG(\sigma) \\ &= f(y), \end{aligned} \quad (31)$$

for $y > 0$. Now, since by assumption G_0 has a regularly varying tail with tail index α_0 , it follows from Theorem 3 that V has a regularly varying tail with tail index α_0/D . Now, let $V_0 \sim G_0$ and $\mathcal{L}^*(\sigma) = \{\mathcal{L}(\sigma)\}^{1/D}$ and note that the assumptions along with Theorem 3 and the representation theorem imply $E(U_+^{\alpha_0}) < \infty$,

$$P(V > \sigma) = \sigma^{-\alpha_0/D} \mathcal{L}^*(\sigma), \quad P(U_+ > \sigma) = o\{P(V_0 > \sigma)\}^{1/D} = o\{P(V > \sigma)\},$$

as well as that

$$\lim_{\sigma \rightarrow \infty} \mathcal{L}^*(\sigma) = \left\{ \lim_{\sigma \rightarrow \infty} \mathcal{L}(\sigma) \right\}^{1/D} > 0.$$

In other words, the assumptions of the extended Breiman's lemma apply from where it readily follows that U_+V is regularly varying at infinity with tail index α_0/D , and hence the same claim can be made about $f_{U_+V}(y) = f(y)$. This proves the result.

b) Let $i(h)$ be a permutation such that $\inf\{\alpha : G_0(\alpha) > 0\} \equiv \alpha_{i(1)} \leq \alpha_{i(2)} \leq \dots$. Then,

$$1 - F(y) = \sum_{h=1}^{\infty} \pi_h \frac{\mathcal{L}(y)}{y^{\alpha_h}} = \sum_{j=1}^{\infty} \frac{\pi_{i(j)} \mathcal{L}(y)}{y^{\alpha_{i(j)}}} = \frac{\mathcal{L}^*(y)}{y^{\alpha_{i(1)}}},$$

and it can be easily shown that $\mathcal{L}^*(y) = \mathcal{L}(y) \{ \pi_{i(1)} + \sum_{j=2}^{\infty} \pi_{i(j)} / (y^{\alpha_{i(j)} - \alpha_{i(1)}}) \}$ is a slowly varying function, from where the final result follows. \square

Proof of Theorem 5: We only present the proof of Theorem 5 a) as that of claim b) follows a similar line of attack. We start by showing that the marginal distributions F_k are univariate Pitman–Yor mixtures, and then using Theorem 4 it follows that their tails, $1 - F_k$, are regularly varying, for $k = 1, \dots, d$. Let $d\mathbf{y}_{-k} = dy_1 \dots dy_{k-1} dy_{k+1} \dots dy_d$ and note that (12) combined with Fubini's theorem implies that

$$\begin{aligned} f_k(y_k) &= \int_{\mathbb{R}_+^{d-1}} f(\mathbf{y}) d\mathbf{y}_{-k} = \int_{\mathbb{R}_+^{d-1}} \left\{ \int_{\mathbb{R}_+^d} \prod_{j=1}^d K_{\sigma_j}(y_j; \eta_{\sigma_j}) dG(\boldsymbol{\sigma}) \right\} d\mathbf{y}_{-k} \\ &= \int_{\mathbb{R}_+^d} \left\{ \int_{\mathbb{R}_+^{d-1}} \prod_{j=1}^d K_{\sigma_j}(y_j; \eta_{\sigma_j}) d\mathbf{y}_{-k} \right\} dG(\boldsymbol{\sigma}) \\ &= \int_{\mathbb{R}_+^d} K_{\sigma_k}(y_k; \eta_{\sigma_k}) \left\{ \prod_{j=1, j \neq k}^d \int_0^\infty K_{\sigma_j}(y_j; \eta_{\sigma_j}) dy_j \right\} dG(\boldsymbol{\sigma}) \\ &= \int_{\mathbb{R}_+^d} K_{\sigma_k}(y_k; \eta_{\sigma_k}) dG(\boldsymbol{\sigma}) \\ &= \int_0^\infty K_{\sigma_k}(y_k; \eta_{\sigma_k}) dG_k(\sigma_k). \end{aligned}$$

Since by assumption $G_{0,k}(\sigma_k)$ has a regularly varying tail with tail index $\alpha_{0,k}$, it follows from Theorem 4 a) that $1 - F_k$ is regularly varying with tail index $\alpha(F_k) = \alpha_{0,k}/D$, for $k = 1, \dots, d$, from where the final result follows. \square

ACKNOWLEDGEMENTS

The authors thank Isadora Antoniano Villalobos, Vanda Inácio de Carvalho, and Sara Wade for discussions and constructive comments on an earlier version of the paper. The research was supported by the Chilean, Mexican, and Portuguese NSFs through the projects Fondecyt Grant 1220229, ANID–Millennium Science Initiative Program–NCN17 059, PTDC/MAT-STA/28649/2017, and UID/MAT/00006/2019.

REFERENCES

- Applebaum, D. (2009). *Lévy processes and stochastic calculus*. CUP, Cambridge.
- Arbel, J., De Blasi, P., and Prünster, I. (2019). Stochastic approximations to the pitman–yor process. *Bayesian Analysis*, 14(4):1201–1219.
- Ayed, F., Lee, J., and Caron, F. (2019). Beyond the chinese restaurant and pitman-yor processes: Statistical models with double power-law behavior. In *International Conference on Machine Learning*, pages 395–404. PMLR.
- Barrientos, A. F., Jara, A., and Quintana, F. A. (2012). On the support of MacEachern’s dependent dirichlet processes and extensions. *Bayesian Analysis*, 7:277–310.
- Bassetti, F., Casarin, R., and Leisen, F. (2014). Beta-product dependent pitman–yor processes for bayesian inference. *Journal of Econometrics*, 180(1):49–72.
- Beirlant, J., Goegebeur, Y., Segers, J., and Teugels, J. (2004). *Statistics of Extremes: Theory and Applications*. Wiley, Hoboken, NJ.
- Bertoin, J. (1999). Subordinators: Examples and applications. In *Lectures on Probability Theory and Statistics*. Springer, New York.
- Bingham, N. H., Goldie, C. M., Teugels, J. L., and Teugels, J. (1989). *Regular variation*. CUP, Cambridge.
- Bladt, M. and Rojas-Nandayapa, L. (2018). Fitting phase–type scale mixtures to heavy–tailed data and distributions. *Extremes*, 21(2):285–313.
- Boettcher, W. S., Hahn, S. S., and Shaw, G. L. (1994). Mathematics and music: A search for insight into higher brain function. *Leonardo Music Journal*, pages 53–58.
- Buzsaki, G. (2006). *Rhythms of the Brain*. Oxford University Press, Oxford.
- Canale, A., Lijoi, A., Nipoti, B., and Prünster, I. (2017). On the pitman–yor process with spike and slab base measure. *Biometrika*, 104(3):681–697.
- Coles, S. (2001). *An Introduction to Statistical Modeling of Extreme Values*. Springer, London.
- Corradin, R., Canale, A., and Nipoti, B. (2021). Bnpx: An r package for bayesian nonparametric modeling via pitman-yor mixtures. *Journal of Statistical Software*, 100:1–33.
- Denisov, D. and Zwart, B. (2007). On a theorem of breiman and a class of random difference equations. *Journal of Applied Probability*, 44(4):1031–1046.

- Doss, H. and Sellke, T. (1982). The tails of probabilities chosen from a dirichlet prior. *The Annals of Statistics*, 10(4):1302–1305.
- Dunn, P. K. and Smyth, G. K. (1996). Randomized quantile residuals. *Journal of Computational and Graphical Statistics*, 5(3):236–244.
- Embrechts, P., Klüppelberg, C., and Mikosch, T. (1997). *Modelling extremal events for insurance and finance*. Springer, New York.
- Ferguson, T. S. (1973). A Bayesian analysis of some nonparametric problems. *The Annals of Statistics*, 1:209–230.
- Ferguson, T. S. (1974). Prior distributions on spaces of probability measures. *The Annals of Statistics*, 2(4):615–629.
- Frank, M. G. (2009). *Brain rhythms*, pages 482–483. Springer Berlin Heidelberg, Berlin, Heidelberg.
- Ghosal, S. and Van der Vaart, A. W. (2015). *Fundamentals of nonparametric Bayesian inference*. CUP, Cambridge.
- Glen, A. G., Leemis, L. M., and Drew, J. H. (2004). Computing the distribution of the product of two continuous random variables. *Computational Statistics & Data Analysis*, 44(3):451–464.
- Ishwaran, H. and James, L. F. (2001). Gibbs sampling methods for stick-breaking priors. *Journal of the American Statistical Association*, pages 161–173.
- Klimesch, W. (2012). Alpha-band oscillations, attention, and controlled access to stored information. *Trends in Cognitive Sciences*, 16(12):606–617.
- Li, C., Lin, L., and Dunson, D. B. (2019). On posterior consistency of tail index for bayesian kernel mixture models. *Bernoulli*, 25(3):1999–2028.
- Lijoi, A., Prünster, I., and Rigon, T. (2020). The pitman–yor multinomial process for mixture modelling. *Biometrika*, 107(4):891–906.
- Miller, J. W. and Harrison, M. T. (2014). Inconsistency of pitman–yor process mixtures for the number of components. *The Journal of Machine Learning Research*, 15(1):3333–3370.
- Müller, P. and Mitra, R. (2013). Bayesian nonparametric inference—why and how. *Bayesian Analysis*.
- Müller, P., Quintana, F. A., Jara, A., and Hanson, T. (2015). *Bayesian Nonparametric Data Analysis*. Springer, New York.
- Nelsen, R. B. (2006). *An introduction to copulas*. Springer series in statistics. Springer, New York, 2nd ed edition.
- Ombao, H., Lindquist, M., Thompson, W., and Aston, J. (2016). *Handbook of neuroimaging data analysis*. Chapman and Hall/CRC, Boca Raton, FL.
- Pitman, J. and Yor, M. (1997). The two-parameter Poisson-Dirichlet distribution derived from a stable subordinator. *The Annals of Probability*, pages 855–900.

- Quintana, F. A., Müller, P., Jara, A., and MacEachern, S. N. (2022). The dependent dirichlet process and related models. *Statistical Science*, 37(1):24–41.
- Resnick, S. I. (2007). *Heavy-tail phenomena: probabilistic and statistical modeling*. Springer, New York.
- Roberts, J. A., Boonstra, T. W., and Breakspear, M. (2015). The heavy tail of the human brain. *Current Opinion in Neurobiology*, 31:164–172.
- Rodu, J. and Kafadar, K. (2022). The q–q boxplot. *Journal of Computational and Graphical Statistics*, 31(1):26–39.
- Sarabia Alegría, J. M., Gómez Déniz, E., et al. (2008). Construction of multivariate distributions: A review of some recent results. *SORT*, 32:3–36.
- Sato, K.-I. (1999). *Lévy processes and infinitely divisible distributions*. CUP, Cambridge.
- Teh, Y. W. (2006). A hierarchical bayesian language model based on pitman–yor processes. In *Proceedings of the 21st International Conference on Computational Linguistics*, pages 985–992.
- Tressou, J. (2008). Bayesian nonparametrics for heavy tailed distribution. Application to food risk assessment. *Bayesian Analysis*, 3(2):367–391.
- Walker, S. G. (2007). Sampling the dirichlet mixture model with slices. *Communications in Statistics—Simulation and Computation*, 36(1):45–54.
- Wang, H. and Tsai, C.-L. (2009). Tail index regression. *Journal of the American Statistical Association*, 104(487):1233–1240.